PATH FOLLOWING FOR THE F18-HARV AIRCRAFT

Costin ENE[1]

A path following algorithm entitled "Nonlinear Guidance Logic" was implemented and tested on the full nonlinear dynamics of the F-18 HARV aircraft. This paper offers a brief description of the algorithm that uses as a main feature an element of anticipation which allows tight tracking of trajectories of different form including circular trajectories. The algorithm uses lateral acceleration generated through the bank angle in order to achieve tracking. A lateral-directional gain scheduler controller is computed for the linearized model in order to control the bank angle. A full nonlinear simulation within a turbulent atmosphere shows that the Nonlinear Guidance Logic achieves great tracking performance of the desired trajectory.

Keywords: Nonlinear Guidance Logic, trajectory tracking, lateral-directional dynamics, high alpha, coordinated turn.

1. Introduction

Path following is an important problem for every aerial vehicle, regardless of the task they are designed for, starting from small drones, UAV's, satellites or large passenger aircraft. When dealing with military aircraft the demands are much higher, thus, the path following needs to be done with precision.

Usually, achieving the desired tracking is done by separating the vehicle guidance and control problems into an outer guidance loop and an inner control loop. The outer guidance loop can be addressed, by using linear proportional and derivative controllers for example. When the two loops are treated simultaneously modern design techniques can be applied such as neural network based adaptive control [1] or receding horizon [2].

The algorithm used for the F18-HARV in order to achieve path following treats the control loop and the guidance loop separately. Using a PID controller will work relatively well when the input commands are step type commands, however if one wants to accurately follow curved trajectories, the PID controllers will achieve tracking with a relatively large error. For example if one would like to follow a sinusoidal type command, the PID will achieve tracking having the output of the same type, a sinusoidal response, but usually of smaller amplitude and having a significant phase difference. The authors in [3] showed that exact tracking of the sinusoidal command can be achieved if one knows the exact

[1] Assistant Teacher, Dept. "Nicolae Tipei" , University POLITEHNICA of Bucharest, Romania, e-mail: ene.costin27@gmail.com

frequency of the sinusoidal command by designing the controller using $\frac{1}{s^2+\omega_n^2}$, (ω_n being the frequency of the sinusoidal command) instead of the common integrator $\frac{1}{s}$. They also provide a solution when one wants to exact follow a ramp type command.

This paper will focus on the algorithm presented in [4], called nonlinear guidance logic, which is based on proportional navigation [5],[6] and uses an imaginary point moving along the desired flight path as a pseudo target in order to achieve trajectory following. The proportional navigation technique is widely used because it ensures satisfactory performance. An important element in proportional navigation is using the fact that the line of sight between a missile and a target constantly changes, also it assumes constant velocity when intercepting.

The guidance logic developed by the authors in [4] has the following features:

- It contains proportional and derivative controls on cross-track error
- It has an element of anticipation → enables tracking of curved trajectories with increased accuracy
- It uses the instantaneous speed of the vehicle → allows adaption with respect to the vehicle inertial speed that can be influenced by external disturbances such as wind.

This paper purpose is to implement the algorithm developed in [4] on the nonlinear dynamics of the F18-HARV. In the chapters to come, a short description of the algorithm will be presented, and then simulations will show the effectiveness of the proposed method. Path following results achieved by the F-18 HARV presented in Chapter 3, include an altitude hold controller, a velocity controller and also a trajectory tracking controller. In this paper one will only focus on the lateral channel, although the final simulation results contain all mentioned above.

2. Guidance logic strategy

Firstly the desired trajectory must be pre-established. The algorithm selects a reference point on the desired trajectory and generates a lateral acceleration command using the reference point.

The reference point is selected at a distance D_1, forward of the vehicle as can be seen in Fig. 1, where the reference point is marked with a green X.

The lateral command acceleration is given by:

$$a_{s_{cmd}} = 2\frac{V^2}{D_1}\sin(\eta) \tag{1}$$

The direction of the acceleration depends on the sign of the angle between the D_1 line segment and the vehicle velocity vector. Notice that in Fig. 1. the reference point is on the right of the aircraft, thus the aircraft will accelerate to the right tending to align its velocity direction with the D_1 line segment.

At each time a circular path can be defined between the vehicle position and the reference point which is tangential to the aircraft velocity vector V, marked with a green dotted line in Fig. 1.

The acceleration command required for the velocity to align with the D_1 line segment is the centripetal acceleration required to follow the circular path.

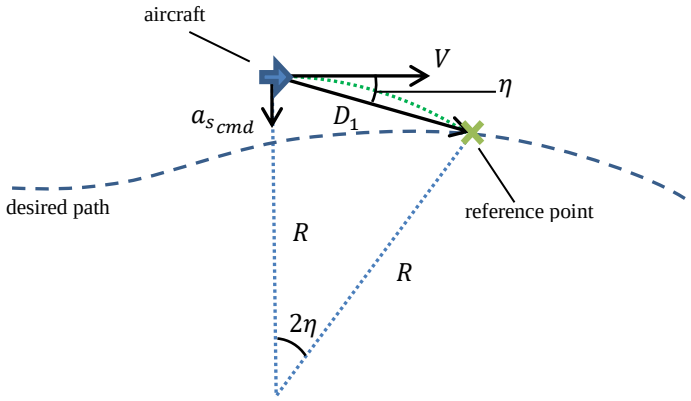

Fig. 1. Diagram for Guidance Logic

In Fig.1. one can notice that

$$\sin(\eta) = \frac{D_1}{2R}. \tag{2}$$

The centripetal acceleration (a_c) is given by $a_c = \frac{V^2}{R}$ and by replacing R from the above equation yields

$$a_c = \frac{V^2}{\frac{D_1}{2\sin(\eta)}} = 2\frac{V^2}{D_1}\sin(\eta) = a_{s_{cmd}}. \tag{3}$$

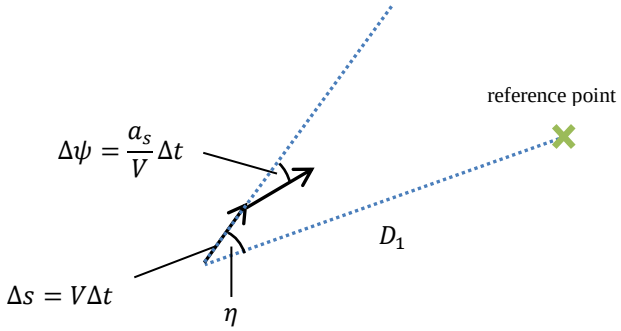

Fig. 2. One time step

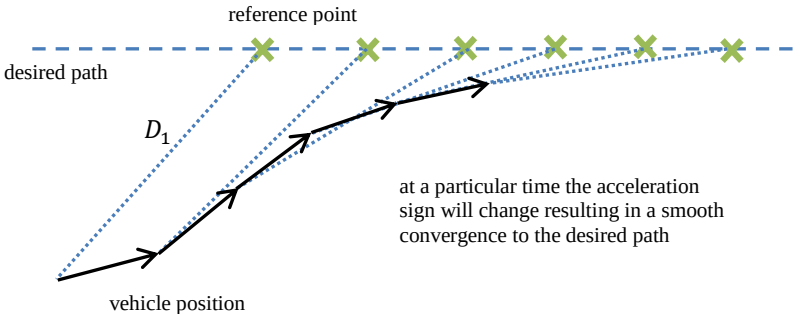

Fig. 3. Step by step representation

Fig. 2. shows the evolution of the guidance logic for one time step. One can see that the vehicle rotates with the yaw angle $\Delta\psi$ in order for the velocity vector to align itself with the line segment D_1. Δs is the distance traveled by the aircraft in one time step Δt.

Fig. 3. shows the trajectory of the vehicle for several time steps. One can see that the vehicle starts from a location far away from the desired path and eventually converges to it.

Two important aspects:

- If the vehicle is far away from the desired path → the vehicle is rotated so that its velocity direction approaches the desired path at a large angle.
- If the vehicle is close to the desired path → the vehicle is rotated so that its velocity direction approaches the desired path at a small angle.

Here one will discuss only the straight line following case. More details regarding the perturbed non-straight line, or when following a circular path can be found in [4].

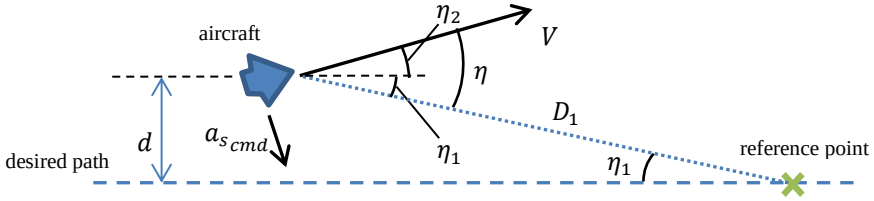

Fig. 4. Straight line following case

In Fig. 4. one has:

- D_1 – the distance from the vehicle to the reference point marked with an X

- d – the cross-track error
- V – the vehicle nominal speed

η is assumed to be small in magnitude, therefore

$$\sin(\eta) \cong \eta_1 + \eta_2 \tag{4}$$

and

$$\eta_1 \cong \frac{d}{D_1},\ \eta_2 \cong \frac{\dot{d}}{V}. \tag{5}$$

Thus replacing the above equations into the lateral command acceleration formula it results that

$$a_{s_{cmd}} = 2\frac{V^2}{D_1}\sin(\eta) \cong 2\frac{V^2}{D_1}\left(\frac{d}{D_1} + \frac{\dot{d}}{V}\right) \cong 2\frac{V}{D_1}\left(\dot{d} + \frac{V}{D_1}d\right), \tag{6}$$

which is a PD controller for the cross-track error. The ratio $\frac{V}{D_1}$ is an important factor that determines the proportional and derivative controller gains. Assuming there are no inner-loop dynamics and also assuming η_2 to be small, then $a_{s_{cmd}} \cong -\ddot{d}$, and equation (6) can be rewritten to obtain:

$$\ddot{d} + 2\zeta\omega_n\dot{d} + \omega_n^2 d = 0, \tag{7}$$

where $\omega_n = 2\frac{V^2}{D_1^2}$ and $\zeta = \frac{1}{\sqrt{2}} = 0.707$.

This results for ω_n and ζ are very important because as can be seen in [4], similar results, with some small particularities are obtained also in the cases when following a perturbed non-straight line, or when following a circular path.

The implementation can be done by considering that the bank angle, ϕ will be used to generate lateral acceleration for the aircraft. Assuming that the vehicle maintains sufficient lift to balance weight, even when banked at angle ϕ, requires that the vehicle speeds up or change the its angle of attack to a larger value.

The lift increment is

$$\Delta C_L = \frac{\mathrm{L}-mg}{\bar{q}S} = (1-n)\frac{mg}{\bar{q}S}, \tag{8}$$

where $n = \frac{L}{mg}$ is the load factor, m is the aircraft mass, S is the wing area, $\bar{q}$ is the dynamic pressure and g is the gravitational acceleration.

Assuming that $\mathrm{L}\cos(\phi) = mg$ and $\mathrm{L}\sin(\phi) = ma_{s_{cmd}}$ it results that

$$\tan(\phi) = \frac{a_{s_{cmd}}}{g} \tag{9}$$

3. Numerical implementation

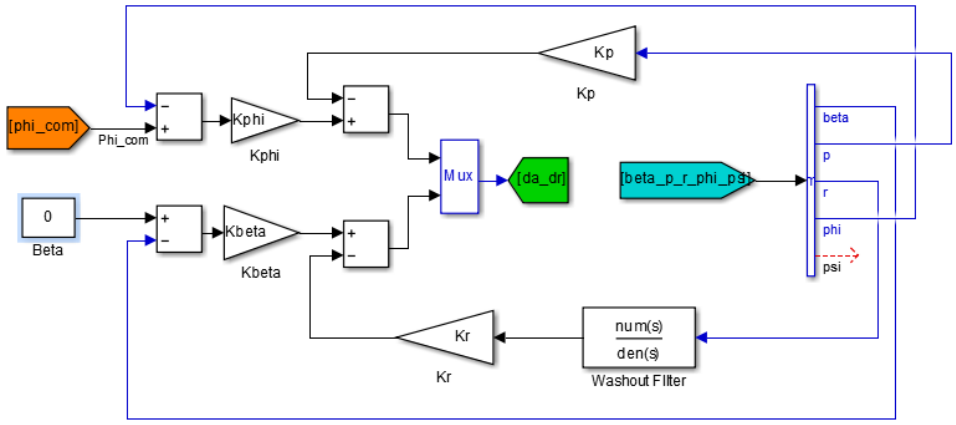

Fig. 5. Lateral-directional controller used for the dynamics of the F-18 HARV aircraft

The linearized lateral-directional dynamic of the F-18 HARV obtained for $\text{TAS} = 500\ \left[\frac{ft}{s}\right],\ \Theta = 5\ [deg],\ \text{H} = 19000\ [ft]$ from [7], are given by:

$$\begin{bmatrix}\dot{\beta}\\ \dot{p}\\ \dot{r}\\ \dot{\phi}\end{bmatrix} = \begin{bmatrix}-0.1306 & 0.087593 & -0.99878 & 0.064348\\ -7.3707 & -1.5884 & 0.56317 & 0.000\\ 1.0342 & -0.00096835 & -0.1162 & 0.000\\ 0 & 1 & 0.087489 & 0.000\end{bmatrix}\begin{bmatrix}\beta\\ p\\ r\\ \phi\end{bmatrix} + \begin{bmatrix}-0.0049739 & 0.0234\\ 11.456 & 1.2614\\ -0.23671 & -0.88607\\ 0 & 0\end{bmatrix}\begin{bmatrix}\delta_a\\ \delta_r\end{bmatrix} \tag{10}$$

First one will show the steps for computing the gains of the gain scheduler controller using root locus. The initial location of the poles is marked by a red square, while the final position after applying the gain is marked with a green diamond.

In order to control the yaw rate one must use a washout filter. Choosing the time constant of the filter to be 4 sec one obtains the following filter structure:

$$K_{wash}(s) = \frac{4s}{4s+1}. \tag{11}$$

From the system in (10) one has the transfer function from the ruder δ_r input to the yaw rate r of the following form:

$$\frac{r(s)}{\delta_r(s)} = \frac{-0.88607\ (s+1.4)(s^2+0.2925s+0.271)}{(s+1.431)(s+0.003871)(s^2+0.4s+1.507)}. \tag{12}$$

This transfer function above is connected in series with the washout filter structure $K_{wash}(s)$, and after that one can apply root locus by changing the sign, cause the resulted transfer function will be negative.

From Fig. 6.(a) one chooses $K_r = -1.6$, and feeds back r multiplied with $K_r K_{wash}(s)$ to the input δ_r of the initial system.

After the above steps, the aileron deflection to roll rate transfer function is:

$$\frac{p(s)}{\delta_a(s)} = \frac{11.456\ (s+0.8499)(s+0.5368)(s+0.4732)(s-0.00552)}{(s+1.519)(s+0.6575)(s+0.001892)(s^2+1.31s+1.061)}. \tag{13}$$

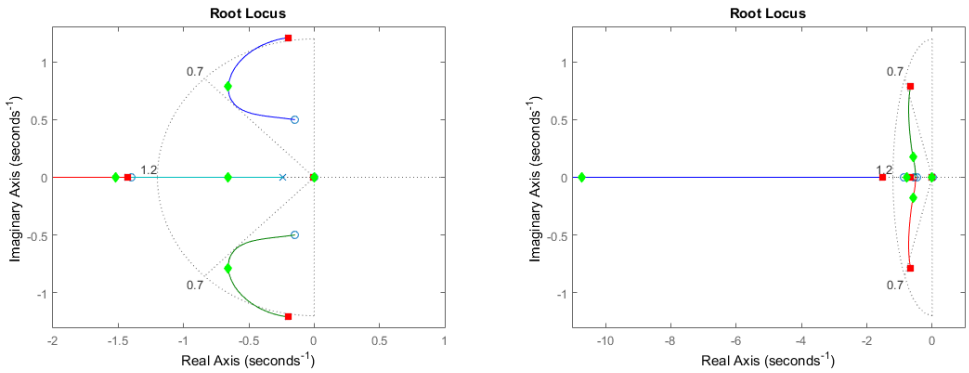

(a) Feedback $K_r K_{wash}(s)$ to δ_r (b) Feedback K_p to δ_a

Fig. 6. Design of the gain scheduler controller used for the lateral-directional dynamics of the HARV-F18 aircraft

One chooses $K_p = 0.8$, as can be seen in Fig. 6 (b) and feeds back pK_p to the aileron input δ_a. The transfer function from the aileron input to the roll angle output is:

$$\frac{\phi(s)}{\delta_a(s)} = \frac{11.435\ (s+0.8401)(s^2+1.014s+0.2578)}{(s+10.73)(s+0.7658)(s-0.002944)(s^2+1.63s+0.3686)}. \tag{14}$$

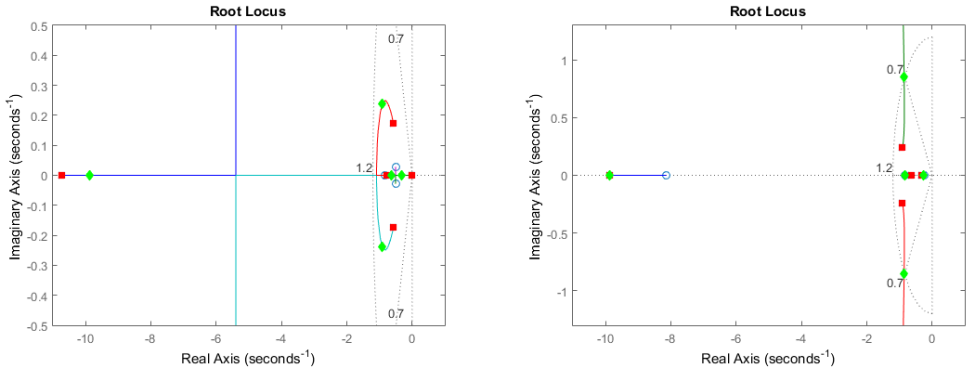

(a) Feedforward K_ϕ to δ_a (b) Feedforward K_β to δ_r

Fig. 7. Design of the gain scheduler controller used for the nonlinear dynamics of the HARV-F18 aircraft

One chooses $K_\phi = 0.729$ to feedforward the roll angle ϕ to the aileron input δ_a.

The transfer function from the rudder input to the sideslip angle output is:

$$\frac{\beta(s)}{\delta_r(s)} = \frac{0.0234\ (s+44.64)(s+8.145)(s+0.8429)(s+0.24)}{(s+9.882)(s+0.6313)(s+0.3259)(s^2+1.818s+0.8839)} \tag{15}$$

One chooses $K_\beta = 0.81$ to feedforward the sideslip angle β to the rudder input input δ_r.

Finally one obtains the lateral-directional gain scheduled control system which meets the Level 1 flying and handling qualities, apart from the spiral mode time constant T_s, which is made much faster.

After designing the lateral roll angle controller one can use the result from (9) in order to develop ϕ_{com} and use it in the roll controller from Fig. 5.

A similar gain scheduler controller was developed in [7] in order to hold the altitude and the forward velocity for the longitudinal channel.

The desired path in earth coordinates (x_{ep}, y_{ep}) consists of a circular part and then a square. The height z_{ep} was also commanded to have a constant decrease of 15 ft/s for the most part of the simulation, then for a short period the aircraft is commanded to fly level, after which, in the last 100 sec. the aircraft is commanded to increase its altitude with 30 ft/s. Total simulation time is 1000 sec. The velocity of the aircraft is maintained such that the path will always be ahead of the aircraft. A wind model containing horizontal wind, shear wind and Dryden turbulence model was included in the simulation, but the turbulence was set to minimum, such that its effect will be noticeable only when the aircraft reaches the altitude of around 7500 ft, at approximately the moment when it is

commanded to fly level. The model on which the simulation was made is the full nonlinear model of the F-18 HARV, in which the lateral controller was kept exactly as constructed above, but the longitudinal controller was also augmented with an L_1 short period controller. During the simulation the speed decreases from $500\ ft/s$ to around $200\ ft/s$ such that the angle of attack will be inside the interval $\alpha \in [5° - 35°]$. D_1 was chosen $2000\ ft$. The path was cheated with a time step of 1 sec., while the simulation pace was set to 0.02 sec.

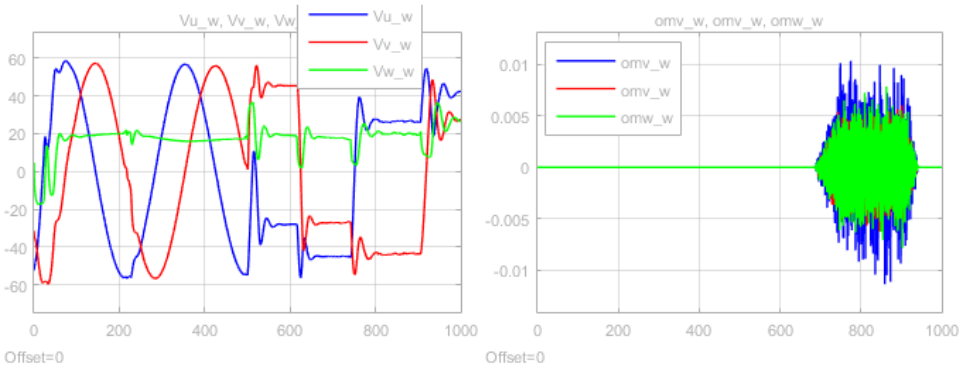

(a) wind velocities + turbulence (b) wind angular velocities + turbulence

Fig. 8. Wind model used for the simulation

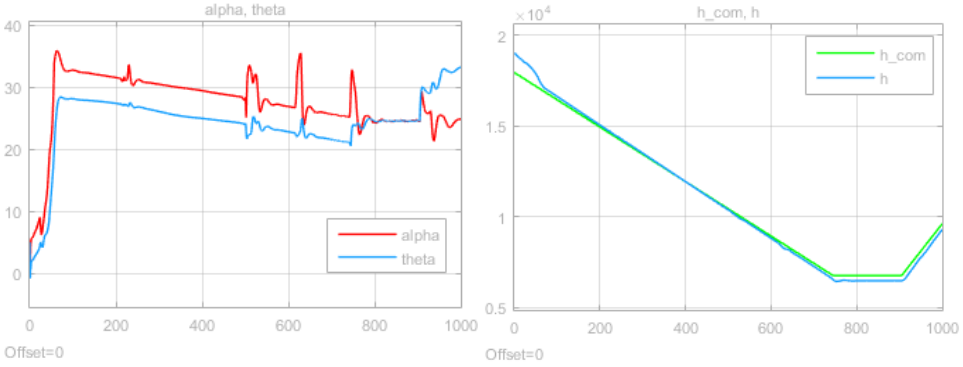

(a) angle of attack α and pitch angle θ (b) response of the commanded altitude H

Fig. 9. Evolution of the angle of attack α, pitch angle θ, and the commanded altitude H

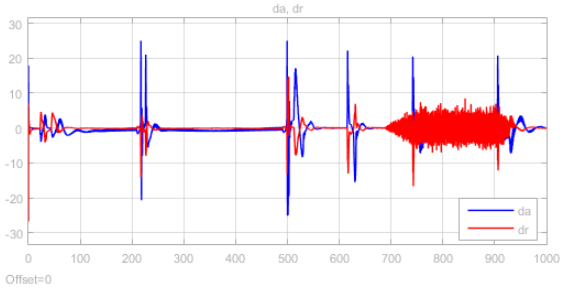

(a) Aileron deflection δ_a and rudder deflection δ_r

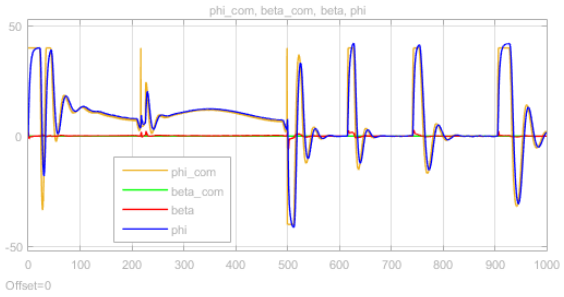

(b) roll angle ϕ and sideslip angle β

Fig. 10. Lateral controller used in the simulation

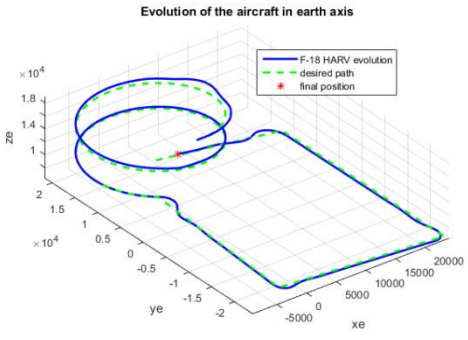

(a)(x_e, y_e, z_e) earth axis view

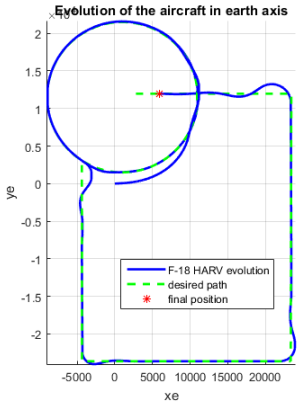

(b) (x_e, y_e) earth axis view

Fig. 11. Path following evolution of the F-18 HARV aircraft

4. Conclusions

The guidance logic worked very well on in the above simulation. It managed to follow the desired part with high accuracy as can be seen clearly in Fig. 11. (b). The aircraft started from position $(0,0,19000)$, while the circular path started from $(1000,1500,19000)$ in the (x_e, y_e, z_e) earth axis coordinates and after around 60 sec the proposed algorithm managed to keep the desired path with an error of approximately $\pm 10ft$, which considering the winds that vary in the interval $\pm 60ft$ is satisfactory.

The altitude controller did not do so well, it lost the commanded altitude with around $300ft$. However this happened at around $H \approx 7500ft$, a flight condition which degrades the performance of this controller by comparison with the initial condition $H_0 = 19000ft$ for which the controller was computed. Also the speed was reduced from $500ft/s$ to approximately $200ft/s$, fact which made the angle of attack rise from $\alpha \cong 5°$ to about $\alpha \cong 35°$, fact which also lowered the controller performance.

The lateral controller worked well and managed to maintain the sideslip angle to approximately $0°$ meaning that the aircraft executed coordinated turns when following the trajectory.

Acknowledgements

The work has been funded by the Sectoral Operational Programme Human Resources Development 2007-2013 of the Romanian Ministry of Labour, through the Financial Agreement POSDRU/107/1.5/S/76909 and by MEN-UEFISCDI Project PN-II-PT-PCCA- 2013-4-1349.

R E F E R E N C E S

[1]. *E. Corban, E. Johnson, and A. Calise*, "A six degree-of-freedom adaptive fight control architecture for trajectory following", in AIAA Guidance, Navigation, and Control Conference and Exhibit, (AIAA-2002-4776), 2002.

[2]. *T. Keviczky and Gary J. Balas*," Software enabled fight control using receding horizon techniques", in AIAA Guidance, Navigation, and Control Conference and Exhibit, (AIAA2003-5671), August 2003.

[3]. *E. J. Davison, A. Goldenberg*, "The robust control of a general servomechanism problem: The servo compensator", in Automatica, **vol. 11**, 1975, pp 461-471.

[4]. *Sanghyuk Park, John Deyst, and Jonathan P. How*, "A New Nonlinear Guidance Logic for Trajectory Tracking", American Institute of Aeronautics and Astronautics, 2004

[5]. *P. Zarchan*, "Tactical and Strategic Missile Guidance", Progress in Astronautics and Aeronautics, **vol. 176**, AIAA, third edition, 1997.

[6]. *J. H. Blakelock*, "Automatic Control of Aircraft and Missiles", Wiley-Interscience, 1991.
[7]. *Costin Ene*, "Application of L_1 adaptive controller to the dynamics of a high maneuverability aircraft" PhD Thesis, University "Polithenica" of Bucharest, 2016